Pulsed Electron Avalanche Knife (PEAK) for Intraocular Surgery

Daniel V. Palanker,[1,2] *Jason M. Miller,*[1] *Michael F. Marmor,*[1] *Steven R. Sanislo,*[1] *Philip Huie,*[1,2] *and Mark S. Blumenkranz*[1]

Purpose. To develop a better and more economical instrument for precise, tractionless, "cold" cutting during intraocular surgery. The use of highly localized electric fields rather than laser light as the means of tissue dissection was investigated.

Methods. A high electric field at the tip of a fine wire can, like lasers, initiate plasma formation. Micrometer-length plasma streamers are generated when an insulated 25 micron (μm) wire, exposed to physiological medium at one end, is subjected to nanosecond electrical pulses between 1 and 8 kV in magnitude. The explosive evaporation of water in the vicinity of these streamers cuts soft tissue without heat deposition into surrounding material (cold cutting). Streamers of plasma and the dynamics of water evaporation were imaged using an inverted microscope and fast flash photography. Cutting effectiveness was evaluated on both polyacrylamide gels, on different tissues from excised bovine eyes, and in vivo on rabbit retina. Standard histology techniques were used to examine the tissue.

Results. Electric pulses with energies between 150 and 670 μJ produced plasma streamers in saline between 10 and 200 μm in length. Application of electric discharges to dense (10%) polyacrylamide gels resulted in fracturing of the gel without ejection of bulk material. In both dense and softer (6%) gels, layer by layer shaving was possible with pulse energy rather than number of pulses as the determinant of ultimate cutting depth. The instrument made precise partial or full-thickness cuts of retina, iris, lens, and lens capsule without any evidence of thermal damage. Because different tissues require distinct energies for dissection, tissue-selective cutting on complex structures can be performed if the appropriate pulse energies are used; for example, retina can be dissected without damage to the major retinal vessels.

Conclusions. This instrument, called the Pulsed Electron Avalanche Knife (PEAK), can quickly and precisely cut intraocular tissues without traction. The small delivery probe and modest cost make it promising for many ophthalmic applications, including retinal, cataract, and glaucoma surgery. In addition, the instrument may be useful in nonophthalmic procedures such as intravascular surgery and neurosurgery. (*Invest Ophthalmol Vis Sci.* 2001;42:2673–2678)

From the [1]Department of Ophthalmology, School of Medicine and [2]W. W. Hansen Experimental Physics Laboratory, Stanford University, Stanford, California.

Supported in part by National Institutes of Health Grant 1 R01 EY12888-01A1 and by Stanford University Incentive Fund.

Submitted for publication January 30, 2001; revised May 24, 2001; accepted May 31, 2001.

Commercial relationships policy: C (DVP, MSB); P (DVP); R (DVP); N (all others).

The publication costs of this article were defrayed in part by page charge payment. This article must therefore be marked "*advertisement*" in accordance with 18 U.S.C. §1734 solely to indicate this fact.

Corresponding author: Daniel V. Palanker, W.W. Hansen Experimental Physics Laboratory, Stanford University, Stanford, CA, 94305-4085. palanker@stanford.edu

The increasing number of microsurgical procedures within the eye places a premium on the development of precise, safe, versatile, and cost-effective instrumentation. The search for improved microsurgical tools has led to the development of diverse mechanical, ultrasonic, electrical, and laser-based devices that facilitate the quality of existing procedures and allow for the execution of new, more advanced surgical maneuvers.

At present the most precise tractionless and nontraumatic ophthalmic microsurgical dissections are carried out with short-pulsed (10^{-9} to 10^{-12} seconds), laser-based instruments (e.g., Nd:YAG, Nd:YLF, and Ti:Sapphire).[1–3] These lasers produce optical breakdown of the transparent medium resulting in plasma formation in the focal area of the laser beam. Temperatures within the plasma volume reach a few thousands degrees, and pressures reach several kBar, so that tissue is rapidly ionized, evaporated, and disintegrated.[4,5] High temperatures and pressures associated with plasma formation allow for dissection of both soft and rigid tissue.

However, this approach of focusing the short-pulsed laser light through the ocular media is limited by the potential hazard to photosensitive tissue caused by intense pulses of light propagating beyond the focal point of the beam.[1,6] In addition, large optical aberrations, for example, while operating on peripheral retina, may increase focal spot size and, consequently, threshold energy, thus reducing the precision and safety of the procedure. Optical breakdown-based ablation is also limited by the need for high optical quality of the liquid–air interface essential for tight focusing of the laser beam inside the organ of interest. Finally, short-pulsed lasers are very expensive and require a cumbersome transport system for preserving the high quality of the laser beam.

Another approach to tractionless and "cold" tissue dissection in fluids is more invasive and is based on application of the pulsed, shallow-penetrating lasers delivered into the eye via optical fibers.[7–9] Fast overheating of a shallow layer of water[10] or tissue[11] by the laser pulse (ns to μs duration) results in formation of a vapor bubble and disruption and ablation of tissue.[10,11] Because the vapor bubble cools down very rapidly (typically in a few microseconds), the effect of this interaction is mainly mechanical, with no detectable thermal damage in the lesion.[12] The main advantage of such systems, compared with the lasers focused from outside the eye (Nd:YAG, Nd:YLF), is that the light is absorbed in a shallow layer adjacent to the tip. Thus, the tissue is treated only in close proximity to the tip and has the same accuracy at any part of the eye and in any direction. Both the Er:YAG[7,8,13] and ArF[9,12] excimer cutting instruments have been used in animal and human intraocular surgery but have failed so far to achieve widespread acceptance in surgical practice because of their prohibitively high cost, large size, and relatively slow pace.[13,14] The pulsed electrosurgical system, which emulates the action of the Er:YAG laser by overheating of the conductive fluid using Joule heat, has been proposed[15] but was found to be limited to use only for very soft tissues such as retina. Our system, which uses an electric field to generate the plasma, eliminates many of these problems.

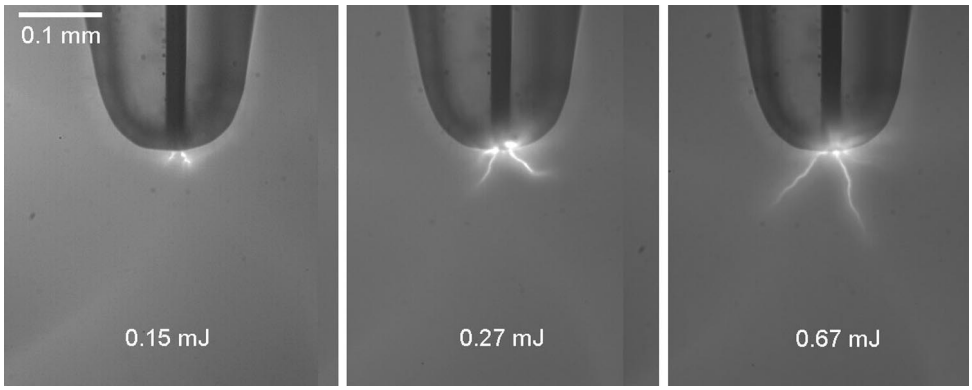

FIGURE 1. Plasma streamers in front of the 25-μm electrode in saline resulting from application of positive pulses of 150-nsec duration. The width of the plasma streamers is ~2 μm, whereas the length varies between 20 and 200 μm. Pulse energy ranges between 150 and 670 μJ.

Plasma generation in liquids allows for deposition of higher energy density than that achieved with light absorption in tissue. This mechanism provides higher temperatures and pressures and thus is more versatile in its applications to surgery of biological tissues. The ideal endosurgical cutter thus would be the one that combines the advantages of powerful but safely confined plasma-mediated interactions and a flexible microprobe delivery with a compact and portable pulse generator of reasonable cost. With such an instrument one could cut tissue efficiently at any point reachable with the microprobe without damaging tissue beyond the close proximity of the tip. We have developed a system, called the Pulsed Electron Avalanche Knife (PEAK), that may achieve these goals by using electricity, rather than laser photons, to generate plasma microstreamers in a conductive aqueous media.

METHODS

Materials and Techniques

Plasma streamers were characterized using a CCD camera (NL/CCD-512; Princeton Instruments, Monmouth Junction, NJ) attached to an inverted microscope (IMT-2; Olympus, Lake Success, NY). Cavitation bubbles were imaged with shadow photography using fast flash (LED, 0.2- to 0.5-μs duration) and a delay generator. Bovine eyes used for testing cutting parameters were obtained from a local slaughter house 3 hours after death. Tissues were cut with the PEAK instrument and then fixed in a 10% formaldehyde solution and embedded in glycomethacrylate plastic (JB-4 Embedding Kit; Polysciences, Inc., Warrington, PA). Sections of selected areas 2 to 3 μm thick were stained with hematoxylin-eosin dye in preparation for light microscopy.

Cutting was also performed on rabbit retina in vivo. Animals were used in accordance with the ARVO Statement for the Use of Animals in Ophthalmic and Vision Research. Two linear cuts approximately 4 mm in length were produced parallel to the medullary ray in each eye after partial vitrectomy. The eyes were enucleated immediately thereafter and fixed in glutaraldehyde/paraformaldehyde fixative, postfixed in osmium tetroxide, and embedded in Epon 812 (Electron Microscopy Sciences, Fort Washington, PA). One-micrometer sections were cut on an ultramicrotome and stained with toluidine blue for light microscopy.

Polyacrylamide gels used for testing cutting parameters were prepared from mixing 6% and 10% (wt/wt) purified polyacrylamide with phosphate-buffered saline (PBS). These gels were polymerized in a Petri dish, which was then loaded onto an inverted microscope stage. Position and orientation of the PEAK probe was controlled using a three-dimensional micromanipulator.

Physical Principles and Instrument Design

Sub-microsecond dielectric breakdown and plasma formation in conductive fluids is a well-known phenomenon that has been studied primarily on the macroscopic (>1 cm) level using two equal-size electrodes in aqueous salt solutions.[16,17] It occurs at electric fields above 10^6 V/cm and a discharge energy density on the order of 1 kJ/cm^3. At such conditions an electron avalanche typically develops during a few tens of nanoseconds.[16] Once the avalanche forms, its interaction with tissue is similar to laser-based dielectric breakdown. Ionization and explosive evaporation of liquid medium can disrupt the adjacent tissue and result in cavitation bubble formation. The high pressures achieved during plasma formation, along with fast expansion (>100 m/sec) of the vapor bubble and subsequent collapse of the cavity, can extend the zone of this interaction beyond the primary energy deposition zone. Because the vapor bubble cools down very rapidly (typically in a few microseconds), the effect of the interaction is mainly mechanical, with no detectable thermal damage to the surrounding tissue.[4,12,18]

To use this process in microsurgery, the size of the plasma-generating electrode must be scaled down to micrometers. Additionally, the plasma discharges must be confined to the probe's tip. We achieved both these goals by designing an asymmetric bipolar microelectrode, so that a micrometer-sized electrode serves as the site of plasma formation, whereas a second, larger electrode is used simply to close the circuit via the conductive physiological medium.

Our plasma-generating electrode (microelectrode) consists of a 25-μm-diameter wire, which is sealed into a tapered insulator and polished to a hemispherical surface at the exit point, as shown in Figure 1. A 4-cm-long concentric steel needle (20 gauge or 0.9 mm OD) surrounds the insulator for mechanical protection and is also used as the second electrode. The internal wire is connected to the output of a high-voltage pulse generator, and the external needle is connected to the common.

The electric field on the tip of the microelectrode is reciprocal to its radius, so that a 25-μm wire allows one to achieve an electric field high enough for plasma generation (>10^6 V/cm) at voltage levels that are transportable by thin flexible cables (several kV). The hemispherical electric field formed around our inlaid microelectrode decreases rapidly with distance ($\sim 1/(r + a)^2$, where a is a radius of the electrode and r is a distance from it). In effect, then, high electric field levels are confined to an area comparable to the electrode's radius. This confinement allows for the generation of micrometer-sized plasma streamers in conductive medium.

RESULTS

Application of sub-microsecond positive pulses via the microelectrode in physiological medium (saline) with voltages above 1 kV (and pulse energies >10 μJ) resulted in formation of narrow plasma streamers (Fig. 1). The width of the plasma streamers (~2 μm) did not change with increasing pulse voltage and energy, but the length extended up to ~200 μm when voltage was increased to 3 kV and energy to 670 μJ. With further increases in pulse energy, the streamers multiplied and branched but did not significantly elongate.

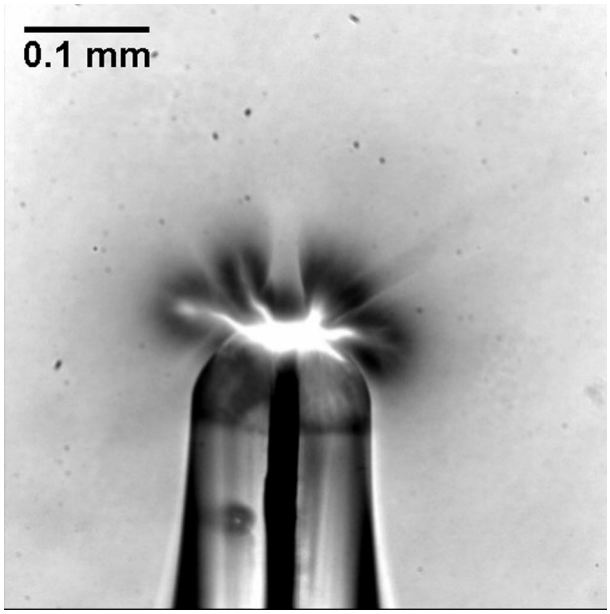

FIGURE 2. Vapor cavities (*dark areas*) forming around each of the plasma streamers in saline 1 μs after the 270-μJ pulse. This shadow photograph was taken on an inverted microscope with a flash of 0.5-μs duration. Approximately 5% of the discharge energy was converted into mechanical energy of the cavitation bubble in our case. The bubble reached a maximal 0.32-mm radius 30 μs after the pulse and then collapsed during the same period. Because of the fast expansion of the bubble (~100 m/sec during the first microsecond) and relatively long flash duration, the boundaries of the vapor cavities look blurred.

Each plasma streamer generated an explosive evaporation of liquid medium, thereby forming multiple vapor cavities, as can be seen in Figure 2. Vapor bubbles growing around each streamer fuse into a spherical bubble, which expands and then collapses, with its lifetime and maximal size dependent on the pulse energy.[19] For example, at a discharge energy of 50 μJ, the bubble reaches a maximal radius of 0.19 mm 16 μs after the pulse and then collapses during the same period. To test the cutting characteristics of PEAK, we used several types of ocular tissue extracted from bovine eyes. The energy requirements and pulse repetition rate that would cut at a practical speed varied greatly among different tissues. For example, we found that to dissect the iris and lens at a rate of 1 mm/sec to a depth of 100 μm/scan, pulse energies of ~500 μJ and a repetition rate of ~50 Hz were required. On the other hand, bovine retina could be dissected in vitreous to full depth (~200 μm) by a single pulse at an energy level of ~90 μJ, with only minor damage to the underlying retinal pigment epithelium cell layer (see Fig. 3). In all these experiments the probe was kept in contact with the tissue. Histologic examination revealed no signs of coagulation at the edges of the crater. With pulses of 50 μJ at a repetition rate of 10 Hz, we could cut bovine retina at a linear rate of 1 mm/sec, while sparing the retinal blood vessels (Fig. 4). At a pulse energy of 90 μJ, large retinal blood vessels could also be incised, which results in bleeding, because PEAK cutting is not accompanied by coagulation.

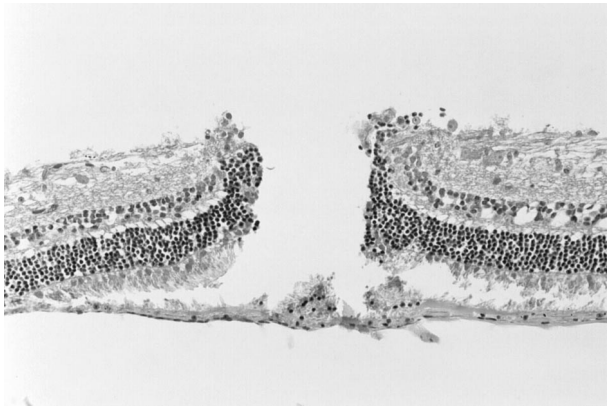

FIGURE 3. Histologic section of a crater in bovine retina resulting from application of one pulse at 90 μJ. A full-depth crater of ~150 μm in width was formed in the retina. Bruch's membrane remained intact, whereas elevation of the retina in the vicinity of the lesion is probably due to the negative pressure gradient formed during collapse of the cavitation bubble. No signs of coagulation or other thermal damage are observed at the edges of the crater.

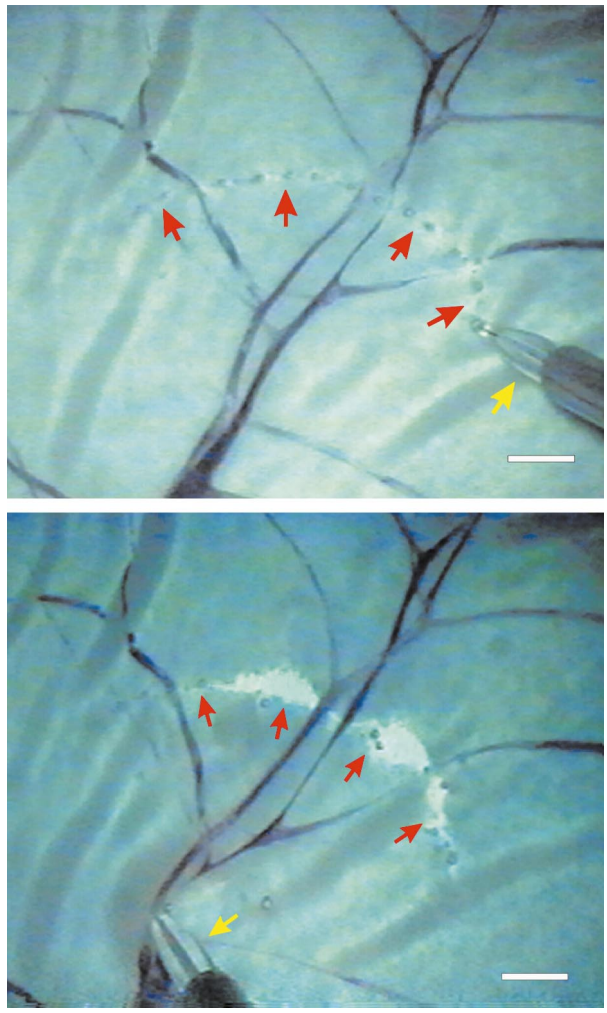

FIGURE 4. Dissection of bovine retina at 50 μJ/pulse with sparing of retinal blood vessels. (**A**) The probe (*yellow arrow*) made a sweep across the retina (*red arrows*) leaving a trail of small gas bubbles. (**B**) The probe is used to pull the retina toward the *left lower corner*, demonstrating a full-depth cut of the retina with preservation of major blood vessels. Scale bar, 1 mm.

Full-depth dissection of rabbit retina in vivo was achieved at a pulse energy of 17 μJ and repetition rate of 10 Hz, with linear cutting rate of 0.5 mm/sec. With this energy level, the cut is not visible clinically but is full-thickness on histology (see Fig. 5). Although retina was fully cut, bleeding from the choroid only occurred at one point along one of four 4-mm-long cuts.

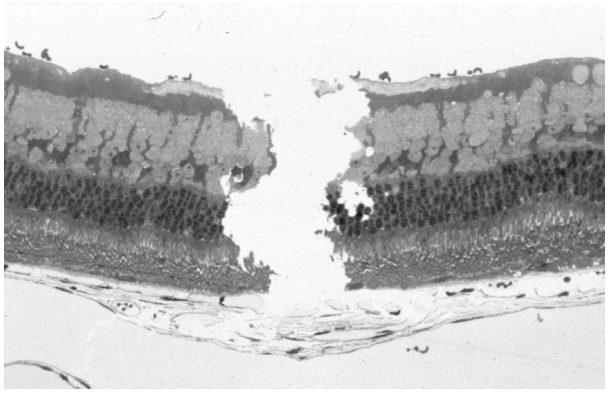

FIGURE 5. Histologic section of the cut in rabbit retina produced with 17-μJ pulses at 10-Hz repetition rate with linear scanning rate of 0.5 mm/sec. Note sharp edges of the cut and absence of coagulation and other thermal damage on the sides of the lesion.

To better evaluate the ability of PEAK to cut tissue at the microsurgical level, we examined its action on polyacrylamide gels of various densities. The transparency of these gels, in contrast to most biological tissue, facilitates imaging and therefore allowed more detailed illustration and characterization of the effects of the instrument. We found that the PEAK's pattern of dissection depended heavily on the density of the gel being cut. Additionally, we found that a 10% gel displayed many of the same cutting properties as the relatively hard tissues in the eye (such as lens capsule and lens cortex). Application of the PEAK instrument to lens capsule or cortex or a 10% gel was quite reproducible and typically produced a cut without ejection of bulk material. (as seen in Fig. 6 for the gel). If no forward movement of the instrument occurred, repetitive pulses were progressively less efficient in deepening the gel's fracture zone, and maximal depth was reached after ~15 pulses (Fig. 6, horizontal sequence). However, the depth of the ruptured zone increased almost linearly with pulse energy (i.e., from 55 μm at 27 μJ to 220 μm at 141 μJ on average), as seen in vertical sequence in Figure 6.

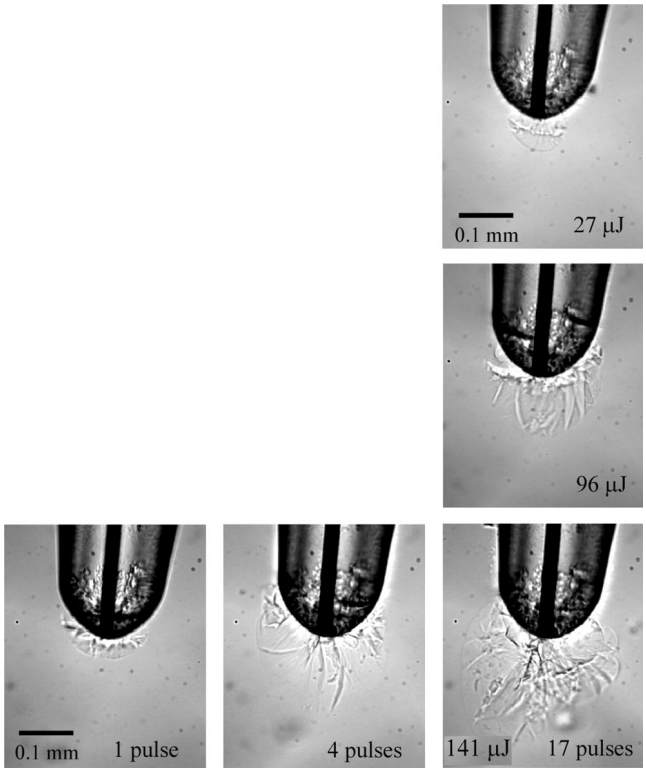

FIGURE 6. Fragmentation of the 10% polyacrylamide gel. The material was placed in a Petri dish and covered with saline. Interaction was observed via an inverted microscope while the microelectrode was held in close proximity to the edge of the gel. Horizontal sequence of frames: growth of the fragmented zone with repeated application of 141-μJ pulses. *Left*: after one pulse; *middle*: after 4 pulses; *right*: frame showing the steady state reached after the application of 15 pulses. Vertical sequence of frames: size of the steady state fragmentation zone ($\geq$15 pulses) increases with increasing pulse energy. *Top*: 27 μJ/pulse, *middle*: 96 μJ/pulse; *bottom*: 141 μJ/pulse.

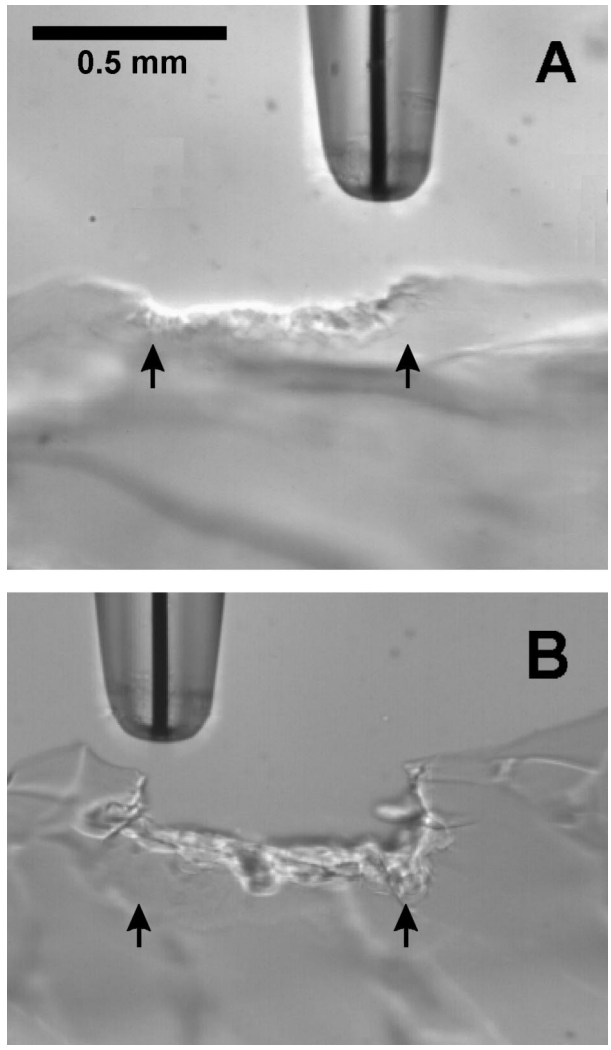

FIGURE 7. Scanning of 6% polyacrylamide gel in saline. Note that unlike the 10% gel shown in Figure 5, the 6% polyacrylamide matrix was not only fragmented but also was ejected. (**A**) Application of 50-μJ/pulse results in 70-μm-deep crater formation. (**B**) Scanning at 96 μJ/pulse produced a 200-μm-deep crater.

Polyacrylamide gel at a 6% concentration shared many of the same cutting properties as softer ocular tissue. Application of PEAK to 6% gel or bovine retina resulted in ejection of the fractured material and formation of a crater. The maximal depth of the crater (saturation level) was still determined by the pulse energy, as shown in Figure 7. Scanning the gel or tissue with forward movement of the probe allowed for removal of the material layer by layer.

Discussion

High-voltage, nanosecond-pulsed electric discharges applied to a micrometer- sized wire can produce plasma microstreamers in physiological medium or in tissue with a diameter of ~2 μm and a length varying between 10 and 200 μm. The high temperatures and pressures associated with these plasma streamers allow for precise dissection of soft tissue without traction, in a fashion similar to the laser-induced dielectric breakdown. Fast expansion of the vapor cavity, formed by high temperatures inside the plasma streamers, causes rapid cooling and mechanical fragmentation of tissue. Histologic examination of cuts made on bovine ocular tissue revealed no collateral thermal damage. Mechanical effects of the plasma–tissue interaction appear to be similar to those observed with optical dielectric breakdown–based instruments.[5]

Because plasma is localized in front of the probe and does not propagate forward as the tissue is removed, pulse energy level is the ultimate determinant of cutting depth. Although increasing the repetition rate increases the speed with which this depth is achieved, the depth of cutting cannot be increased past a saturation point unless the pulse energy is increased. This phenomenon is an important safety feature: inevitable variations in the number of pulses delivered to each point of tissue during surgical dissection using a continuous train of pulses will not result in variation of the cutting depth. Thus, for example, dissection of a pathologic membrane on top of the retina will not result in retinal lesion, regardless of how many pulses are applied, so long as the energy level is set to a crater depth less than the membrane thickness, and the probe is not moved in a forward direction.

We found that fragmentation of a 10% polyacrylamide gel, which mimics the more rigid structures of the eye (thick fibrotic membranes, lens, and lens capsule), is not accompanied by ejection of debris into the surrounding liquid. Importantly, this suggests that PEAK can dissect tissue of similar consistency without contamination of the medium. This effect will be important during intraocular surgery, where continued imaging of tissue through the liquid medium is essential but where the fluid exchange rate is limited.

Efficiency of tissue dissection with PEAK varies considerably with the tissue's mechanical properties. Softer tissue requires fewer pulses and/or lower voltage to achieve the same depth of cut as more rigid tissue. The substantial difference in mechanical strength and in conductivity of different types of tissue makes it possible to perform tissue-selective surgery. For example, retinal tissue (in vitro bovine eyes) can be cut at a pulse energy of ~50 μJ, with no visible damage to the larger retinal blood vessels (see Fig. 4), whereas those can be dissected at pulse energies exceeding 90 μJ. Rabbit retina in vivo is cut at even lower pulse energies: ~17 μJ (see Fig. 5). Because tissue is dissected without substantial heat deposition in the surrounding medium, other modalities such as diathermy may be necessary to control bleeding from cut vessels.

The ability to control crater depth through energy deposited and the number of pulses fired may allow the development of applications such as "shaving" of soft epiretinal membranes adherent to the retina or removal of pathologic or unwanted tissue surrounding a vessel without damaging the vessel itself. The instrument's ability to cut at controlled depth, combined with its capacity for tissue-selective surgery, may eventually allow surgeons a safe, efficient, and bloodless way to remove highly vascularized and tightly adherent epiretinal fibrotic membranes in conditions such as diabetic retinopathy, proliferative vitreoretinopathy, and retinopathy of prematurity.

The instrument's ability to both cut without traction and potentially to "shave" tissue layer by layer makes PEAK potentially useful for cataract surgery as well. Tractionless cutting of the anterior capsule could reduce the incidence of capsule rupture. Layer by layer shaving of the lens material would then allow the surgeon a controlled method for removing the cataract without jeopardizing the integrity of the posterior capsule.

We are currently in the process of testing other ophthalmic applications for the instrument, including scleral shaving to facilitate trans-scleral drug delivery, capsulotomy and lens emulsification, initial dissection of the internal limiting membrane during macular hole surgery, dissection of retinal tissue during radical retinectomy, and modification of the trabecular meshwork in glaucoma surgery. In addition to its use in ophthalmology, PEAK microelectrodes could be attached to thin flexible cables and positioned deep inside the human body to aid in, for example, vascular surgery, neurosurgery, and controlled tumor removal. This technology could replace cumbersome and expensive short-pulsed laser systems in endosurgical applications. Its simplicity and low cost may lead to widespread acceptance in clinical practice if the unique capabilities outlined in this work are confirmed by further preclinical and clinical studies.

Acknowledgments

The authors thank Joost Bakker, Christopher Griffith, Dmitrii Simanovskii, and Alexander Vankov for their help with hardware development and assistance with the experiments as well as Johanna Miller and Roopa Dalal for their help with sample preparations.

References

1. Geerling G, Roider J, Schmidt-Erfurt U, et al. Initial clinical experience with the picosecond Nd:YLF laser for intraocular therapeutic applications. *Br J Ophthalmol.* 1998;82:504–509.
2. Lin CP, Weaver YK, Birngruber R, Fujimoto JG, Puliafito CA. Intraocular microsurgery with a picosecond Nd:YAG laser. *Lasers Surg Med.* 1994;15:44–53.
3. Vogel A, Schweiger P, Frieser A, Asiyo M, Birngruber R. Mechanism of action, scope of the damage and reduction of side effects in intraocular Nd:YAG laser surgery. *Fortschr Ophthalmol.* 1990;87:675–687.
4. Vogel A, Busch S, Jungnickel K, Birngruber R. Mechanisms of intraocular photodisruption with picosecond and nanosecond laser pulses. *Lasers Surg Med.* 1994;15:32–43.
5. Vogel A, Capon MR, Asiyo-Vogel MN, Birngruber R. Intraocular photodisruption with picosecond and nanosecond laser pulses: tissue effects in cornea, lens, and retina. *Invest Ophthalmol Vis Sci.* 1994;35:3032–3044.
6. Cain CP, Toth CA, DiCarlo CD, et al. Visible lesion thresholds from near-infrared pico and nanosecond laser pulses in the primate eye. *Laser-Tissue Interaction VIII, Proc SPIE.* 1997;2975:133–137.
7. Brazitikos PD, D'Amico DJ, Bernal MT, Walsh AW. Erbium:YAG laser surgery of the vitreous and retina. *Ophthalmology.* 1995;102:278–290.
8. Brazitikos PD, D'Amico DJ, Bochow TW, Hmelar M, Marcellino GR, Stangos NT. Experimental ocular surgery with a high-repetition-rate erbium:YAG laser. *Invest Ophthalmol Vis Sci.* 1998;39:1667–1675.
9. Hemo I, Palanker D, Turovets I, Lewis A, Zauberman H. Vitreoretinal surgery assisted by the 193-nm excimer laser. *Invest Ophthalmol Vis Sci.* 1997;38:1825–1829.
10. Lin CP, Stern D, Puliafito CA. High-speed photography of Er:YAG laser ablation in fluid. Implication for laser vitreous surgery. *Invest Ophthalmol Vis Sci.* 1990;31:2546–2550.
11. Palanker D, Turovets I, Lewis A. Dynamics of ArF excimer laser-induced cavitation bubbles in gel surrounded by a liquid medium. *Lasers Surg Med.* 1997;21:294–300.

12. Palanker D, Hemo I, Turovets I, Zauberman H, Fish G, Lewis A. Vitreoretinal ablation with the 193-nm excimer laser in fluid media. *Invest Ophthalmol Vis Sci.* 1994;35:3835–3840.
13. D'Amico DJ, Brazitikos PD, Marcellino GR, Finn SM, Hobart JL. Initial clinical experience with an erbium:YAG laser for vitreoretinal surgery. *Am J Ophthalmol.* 1996;121:414–425.
14. D'Amico DJ, Blumenkranz MS, Lavin MJ, et al. Multicenter clinical experience using an erbium:YAG laser for vitreoretinal surgery. *Ophthalmology.* 1996;103:1575–1585.
15. Palanker D, Turovets I, Lewis A. Electrical alternative to pulsed fiber-delivered lasers in microsurgery. *J Appl Phys.* 1997;81:7673–7680.
16. Jones HM, Kunhardt EE. Development of pulsed dielectric breakdown in liquids. *J Phys D Appl Phys.* 1995;28:178–188.
17. Jones HM, Kunhardt EE. Pulsed dielectric breakdown of pressurized water and salt solutions. *J Appl Phys.* 1995;77:795–805.
18. Wesendahl T, Janknecht P, Ott B, Frenz, M. Erbium:YAG laser ablation of retinal tissue under perfluorodecaline: determination of laser-tissue interaction in pig eyes. *Invest Ophthalmol Vis Sci.* 2000;41:505–512.
19. Turovets I, Palanker D, Lewis A. ArF excimer laser-induced bubble formation during irradiation of NaCl solutions. *Photochem Photobiol.* 1994;60:412–414.